FPCM-9 (2008)
The 9th International Conference on Flow Processes in Composite Materials
Montréal (Québec), Canada
8 ~ 10 July 2008

EXPERIMENTAL STUDY OF FIBER-MATRIX SEPARATION DURING COMPRESSION OF GLASS MAT THERMOPLASTICS

Pierre J.J. Dumont [1,4], Laurent Orgéas [2], Véronique Michaud [3] and Denis Favier [2]

[1] *CNRS / Université de Grenoble, Laboratoire de Génie des Procédés Papetiers (LGP2), 461 rue de la Papeterie, BP 65, 38402 Saint-Martin-d'Hères cedex, France*
[2] *CNRS / Université de Grenoble, Laboratoire Sols-Solides-Structures-Risques (3SR), BP 53, 38041 Grenoble cedex 9, France*
[3] *Laboratoire de Technologie des Composites et Polymères (LTC), École Polytechnique Fédérale de Lausanne (EPFL), Station 12, CH-1015 Lausanne, Switzerland*
[4] *Corresponding Author's Email: pierre.dumont@efpg.inpg.fr*

SUMMARY: The fiber-matrix separation occurring during the compression molding of Glass Mat Thermoplastics (GMT) by compression is investigated by performing lubricated plane strain compression experiments at 200°C. The fiber concentration along the deformed samples was determined by a charring and weighting technique. The influences of process parameters on fiber-matrix separation, such as the initial length of samples, the final compression ratio of samples and the axial strain rate are illustrated and discussed.

KEYWORDS: rheology, fiber-matrix separation, compression, Glass Mat Thermoplastics (GMT), short fiber polymer composites

INTRODUCTION

Glass Mat Thermoplastics (GMT) are widely used in the automotive industry to produce semi-structural parts by compression molding. They are formed of a needled complex fibrous microstructure blended with a thermoplastic matrix. After molding, heterogeneities in the spatial distribution of concentration of fibers can be observed in the produced parts [1,2], similarly to the phenomena that can be observed during the compression molding of Sheet Molding Compounds (SMC) [3] or the injection molding of short fiber reinforced thermoplastic polymers [4]. Despite their potential negative effects on the physical and mechanical properties of produced parts, these phenomena have been scarcely studied experimentally and theoretically for this class of composite materials. One of the key challenges remains thus the determination of the material and process parameters that can induce these phenomena. The influence of some of these process parameters, including the initial length of the samples, the compression strain and the axial strain rate is here investigated experimentally by performing lubricated plane strain compression

experiments at 200°C with industrial GMT. This permits to establish some phenomenological fiber-matrix separation rules.

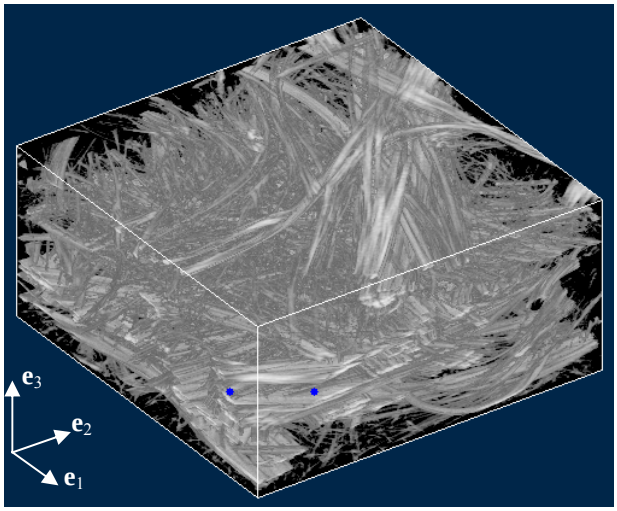

Fig. 1 3D view of the complex fibrous network within a non-deformed GMT sample. This reconstructed micrograph has been obtained with X-ray microtomography (size of the scanned volume 3.9×3.9×2.5 mm^3, beam line ID 19 ESRF, voxel size 7.5 μm).

MATERIALS

The GMT plates studied of initial thickness $h_0 \approx 5$ mm are supplied by Quadrant AG (Switzerland). As shown from the reconstructed 3D micrograph given in Fig. 1, they are made of a high concentration of entangled and needled fiber-bundles displaying a random orientation which is mainly contained in the principal plane ($\mathbf{e}_1$,$\mathbf{e}_2$) of the plates. Fiber bundles are impregnated by a polypropylene matrix (PP). They are composed of approximately 200 glass fibers of diameter 15 μm and have a length of 50 mm. Their initial cross section is elliptical and exhibits major and minor axes close to 80 and 400 μm, respectively. The initial mass fraction of fibers f_0 is homogeneous, *i.e.* $f_0 = 0.33 \pm 0.01$. Besides, the steady state shear viscosity μ of the PP matrix at 200°C was investigated with a parallel plate rheometer (for shear strain rates $\dot{\gamma}$ ranging from 10^{-3} to 10 s^{-1}) and a capillary rheometer (for shear rates ranging from 10 to 10^4 s^{-1}). It follows a non-Newtonian viscous behavior that is well fitted by a Carreau-Yasuda model:

$$\mu = \mu_0 (1 + (\dot{\gamma} / \dot{\gamma}_c)^a)^{(n-1)/a} \tag{1}$$

where the Newtonian viscosity μ_0, the power-law exponent n, the characteristic shear rate $\dot{\gamma}_c$ and the curvature parameter a were set to 160 Pa s, 0.36, 200 s^{-1} and 1, respectively.

EXPERIMENTAL PROCEDURE

Rectangular samples (initial length $L_0 = 80$ mm or 160 mm ($\mathbf{e}_1$-direction) and width $l_0 = 80$ mm ($\mathbf{e}_2$-direction)) were compressed inside a rectangular channel heated at 200 ± 1°C of width $l_0 = 80$ mm, using a specially designed plane strain compression rheometer [5]. This rheometer was mounted on a hydraulic press (Interlaken Tech. Corp. series 3300, 100 kN). Prior the tests, the

surfaces of the sample were coated with a silicone grease layer so that the homogeneity of the sample deformation was ensured during the compression. The current height h of the sample and the current axial compression force F ($\mathbf{e}_3$-direction) were simultaneously recorded during the tests. This allows determining the axial compression ratio $\lambda = h/h_0$ as well as the nominal axial stress $\Sigma = |F|/l_0L_0$. All tests were performed at constant axial velocity v until a final compression λ_f: the initial axial strain rate $D_0 = |v|/h_0$ was varied from 10^{-4} to 10 s^{-1}. At the end of the tests, samples were cooled down to room temperature (20°C). Then, parallel strips (width l_0 and length $\Delta L \approx 10$ mm) were (i) cut from the samples along the flow direction $\mathbf{e}_1$. Using a charring and weighting technique, this permitted to determine the mass fraction of fibers f along the flow direction $\mathbf{e}_1$ of the deformed samples.

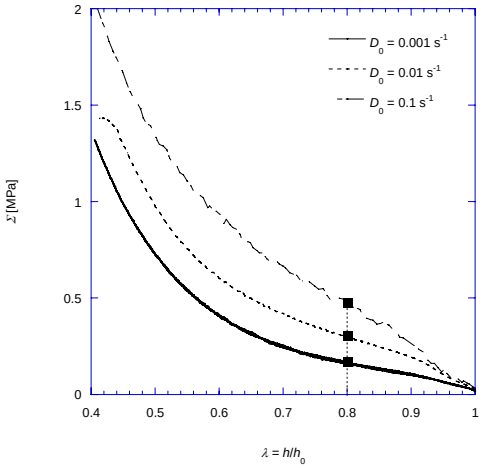

Fig. 2 Typical evolution of the axial nominal stress Σ with respect to the axial compression ratio λ at various initial strain rates D_0.

RESULTS

The graph plotted in Fig. 2 shows typical evolutions of the nominal axial stress Σ with respect to the compression ratio λ for three different initial axial strain rates D_0. Two main features can be observed on all curves: (i) the sharp increase of Σ when decreasing λ, whatever D_0 and (ii) the dependence of Σ with D_0. This latter observation shows a pronounced viscous part in the rheology of the tested GMT's.

The graph given in Fig. 3a reveals the complex shape of the profile of the fiber mass fraction f along the normalized abscissa x_1/L_0 ($x_1 = 0$ corresponding to the centre of samples) measured for various samples having an initial length $L_0 = 80$ mm (final compression ratio $\lambda_f = 0.4$). Three zones are systematically observed in these profiles. In the centre of samples, f exhibits a plateau characterized by a more or less constant fiber content f_p, which is higher than f_0. Near the free surfaces of samples, f is much lower than f_p and f_0. The transition zone in which f rapidly decreases is located between the two previous regions at a normalized abscissa x_p/L_0. These profiles indicate that the fiber mass fraction is heterogeneous along the length of the compresses samples, whatever the imposed axial strain rate D_0. Thus, a systematic separation phenomenon occurs between the polymer matrix and the fibrous network during the compression of GMT.

Graphs also shown in Fig. 3b and 3c emphasize the influences of both the final compression ratio λ_f and the initial length L_0 on the fiber-matrix separation. Some fundamental phenomenological rules can be established from them:

(a) The lower the imposed strain rate D_0, the higher the fiber-matrix separation.

(b) The lower the compression ratio λ_f, the higher the fiber-matrix separation. At high strain rates, this is revealed by the increase of the width of the transition zone as λ_f diminishes (see Fig. 3(b)). At low strain rates, fiber-matrix separation is underlined by the strong increase of f_p with λ_f.

(c) The lower the initial length of samples L_0, the higher the fiber-matrix separation: *e.g.* f_p is systematically higher for smaller samples whatever D_0 (see Fig. 3c).

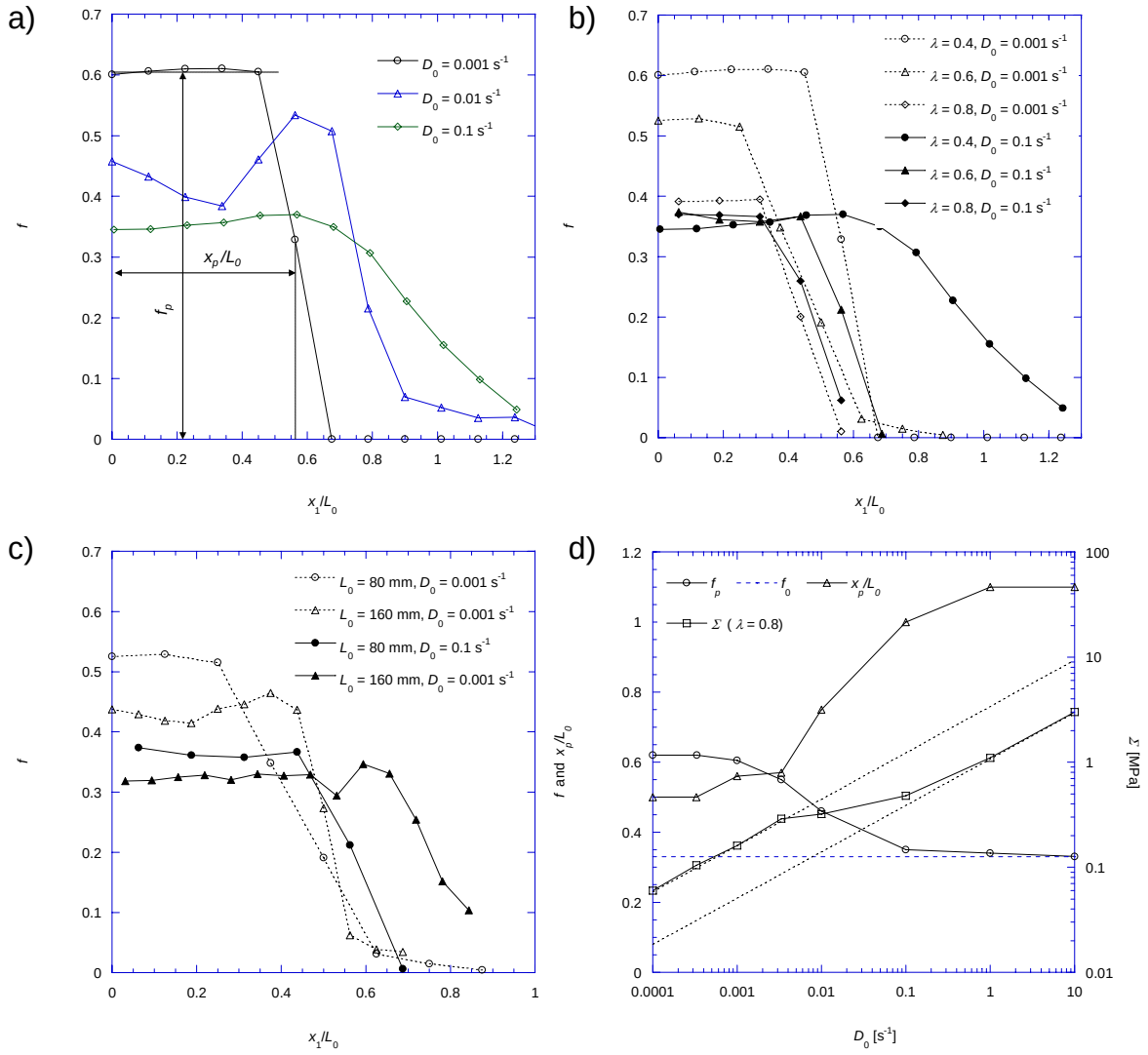

Fig. 3 Evolution of the fiber mass fraction f along the normalized abscissa x_1/L_0 ($\lambda_f = 0.4$, initial sample length $L_0 = 80$ mm): (a) for various initial axial strain rates D_0; (b) various final compression ratios λ_f at various D_0; (c) various initial lengths L_0 at various D_0 ($\lambda_f = 0.6$); (d) evolutions of f_p, x_p/L_0 as well as on the stress levels Σ recorded at $\lambda_f = 0.4$ with D_0.

DISCUSSION AND CONCLUDING REMARKS

The previous results show that the separation phenomenon between the polymer matrix and the fibrous network systematically occurs during the compression molding of the tested GMT. One leading parameter on these phenomena is the initial axial strain rate D_0. Its influence on f_p, x_p/L_0 as well as on the stress levels Σ recorded at $\lambda_f = 0.4$ during compression experiments at $\lambda_f = 0.8$, is emphasized in details in Fig. 3d:

(a) For low values of D_0 ($D_0 \leq 0.001$ s^{-1}), the fiber-matrix separation is pronounced: f_p is much higher than f_0 and x_p/L_0 is very close to 0.5, *i.e.* close to its initial value before compression: fibrous networks have been compressed in the $\mathbf{e}_3$-direction without flowing in the $\mathbf{e}_1$ one (nearly odometric compaction). Hence, the rheology of GMT in this strain rate range is the one of a two-phase medium ("consolidation" regime): (i) the interstitial pressure within the polymer matrix is sufficiently low so that fiber bundles remain entangled and needled and are severely compressed, (ii) the interstitial pressure gradient from the center of samples to their free surface is high enough to induce the migration of the non-Newtonian polymer matrix through the fibrous network.

(b) For high values of D_0 ($D_0 \geq 0.1$ s^{-1}), the fiber-matrix separation is much less pronounced. Indeed, f_p is closer to f_0 and x_p/L_0 reaches values equal to 1.1, showing that fibrous networks flow in the $\mathbf{e}_1$-direction during their compression. The rheology of GMT in this strain rate range tends to that of a one-phase medium ("liquefaction" regime). This also suggests that (i) the interstitial pressure within the polymer matrix is sufficiently high to induce the disentanglement and the relative motion of fiber bundles, (ii) the interstitial pressure gradient is not high enough to induce significant flow of the polymer matrix through the fibrous network.

(c) For values of D_0 between 0.001 s^{-1} and 0.1 s^{-1}, a transition zone between the two previous ones is observed.

(d) Within the "liquefaction" or the "consolidation" regimes, stress levels follow power-laws with an identical power-law exponent of 0.4 (see the two parallel dotted lines sketched in Fig. 2d), which is very close to the one obtained for the polymer matrix above 100 s^{-1} (see the Carreau-Yasuda model). Within the "consolidation" regime, this suggests that microscopic deformation mechanisms occurring at the fiber scale are mainly ruled (i) by the flow of the non-Newtonian polymer through fiber bundles, (ii) by non-Newtonian viscous friction forces at bundle-bundle contacts, this latter mechanism being the only one active within the "liquefaction" regime.

ACKNOWLEDGMENTS

The authors wish to thank the company Quadrant for supplying the GMT and the GDRE "HETerogeneous MATerials" for its financial support. They also gratefully acknowledge Sabine Rolland du Roscoat as well as Jean-Francis Bloch for their scientific and technical support to obtain the micrographs of Fig. 1 at the ESRF.

REFERENCES

1. Y. Yagushi, H. Hojo, D. G. Lee and E. G. Kim, "Measurement of Planar Orientation of Fibers for Reinforced Thermoplastic Using Image Processing", *Int. Polymer Processing*, Vol. 3, 1995, pp. 262–269.

2. P. Dumont, L. Orgéas, C. Servais, V. Michaud, D. Favier, and J.A.E. Månson, "Influence of Material and Process Parameters on Segregation Phenomena During Compression Molding of GMT", in the Pub. House of the Rom. Acad., editor, *Proc. of 8th Int. ESAFORM Conf. on Material Forming*, 2005, pages 975–78.

3. T.H. Le, P.J.J. Dumont, L. Orgéas, D. Favier, L. Salvo and E. Boller, "X-ray Phase Contrast Microtomography for the Analysis of the Fibrous Microstructure of SMC Composites", *Compos. Part A*, Vol. 39, 2008, pp. 91–103.

4. F. Danes, B. Garnier, T. Dupuis, P. Lerendu and T.-P.Nguyen, "Non-Uniformity of the Filler Concentration and of the Transverse Thermal and Electrical Conductivities of Filled Polymer Plates", *Compos. Sci. Technol.*, Vol. 65, 2005, pp. 945–951.

5. P. Dumont, J.-P. Vassal, L. Orgéas, V. Michaud, D. Favier, and J.A.-E. Månson, "Processing, Characterization and Rheology of Transparent Concentrated Fibre Bundle Suspensions", *Rheol. Acta*, Vol. 46, 2007, pp. 639–641.